Available online at www.sciencedirect.com

ScienceDirect

Procedia Structural Integrity 37 (2022) 389–396

Structural Integrity Procedia

www.elsevier.com/locate/procedia

ICSI 2021 The 4th International Conference on Structural Integrity

PU tensile tests: conventional and digital image correlation analysis.

Flaminio C. P. Sales[1,2], Ronaldo M. Ariati[1], Verônica T. Noronha[1], Romeu R. C. da Costa[2], João E. Ribeiro[1],*

[1]ESTiG, Instituto Politécnico de Bragança, 5300-052, Bragança; Portugal; jribeiro@ipb.pt;*
[2]Dept. Eng. Mecânica, UTFPR, Cornélio Procópio, Brazil.

Abstract

Polyurethane (PU) is a polymer, used as coating, paint, foam, adhesive, and even in biomedical devices. To furthermore expand its applications, it can be combined with additives such as Calcium Carbonate ($CaCO_3$), an inexpensive material, widely available in nature, or with fibers, such as glass fibers explored in several sectors, likewise the aerospace and automobile industries. To determine the mechanical properties of these materials, the tensile test is the most used due to its great ease of application and flexibility. However, conventional processes, such as the use of strain gauges or crosshead displacement data, may not provide detailed information about the strain field, or cannot be able to evaluate the Poisson's ratio and the true stresses for the entire stress-strain curve. Thus, digital image correlation (DIC) methods are a promising alternative, consisting of strain field measurement without contact with the surface of the structure. In this context, this study carried out the tensile characterization of two main polyurethane samples: one petrochemical, distributed by Sika®, reinforced with type E glass fiber: and the other, natural, manufactured by Kehl® from castor oils, and combined with CaCO3 particles. During the tests, DIC was applied to evaluate the Poisson's ratio and, subsequently, Scanning Electron Microscopy (SEM) analyses were performed, revealing a higher number of bubbles on Sika's polymer, which contributes to the reduction of the maximum supported stresses, since these pores, with dimensions of up to 25 µm, were regions where the cracks started and headed the breakage. Poisson's ratios were all around 0.4 and the highest tensile strength values were obtained from E-glass reinforced samples (TS015), around 117.24 ± 13.20MPa. $CaCO_3$ particles also acted as reinforced, increasing maximum stress reached from 20MPa to values between 29 and 37MPa.

Keywords: PDMS; Tensile Test; Hardness Test.

1. Introduction

Polyurethane (PU) is an extremely versatile polymer, formed by the addition reaction between isocyanates and polyols, and obtained from natural or petrochemical sources (Da Costa et al., 2017). Furthermore, it can be synthesized

10.1016/j.prostr.2022.01.100

as thermoplastic or thermoset and has characteristics such as low cost, elasticity, and high tensile, impact, abrasion and corrosion resistance. These features make it to be widely applied, being used as coating, paint, foam, adhesive, and even in biomedical devices (Charlon et al., 2014; Chattopadhyay and Raju, 2007; Fu et al., 2015; Lin et al., 2021; Wang and Wang, 2012). Thus, since 1967 it has been applied as a biomaterial, as it has good mechanical characteristics and biocompatibility (Boretos and Pierce, 1967; George and Suchithra, 2019).

It can also be used with additives such as Calcium Carbonate ($CaCO_3$), an inexpensive material, widely available in nature and already used as a reinforcement for bone structures and orthodontic restorations (de Moura et al., 2021; Gao et al., 2011).

Another alternative is the use of PU in composites, with emphasis on glass fiber reinforced materials, explored in several sectors, such as the aerospace and automobile industries (Reis et al., 2013; Soric et al., 2008). This reinforcement has low cost, wide availability, high rigidity and mechanical resistance (Sathishkumar et al., 2014). Moreover, cytotoxicity tests have reached satisfactory results with E-type glass fibers, not showing severe inflammatory reactions when implanted in rats (Lazar et al., 2016).

To determine some mechanical properties of these materials, the tensile test is the most used due to its great ease of application and the flexibility of the method (Garcia, 2012; Sales et al., 2021). However, conventional methods, such as the use of strain gauges or crosshead displacement data, may not provide detailed information about the strain field, or be unable to calculate the Poisson's ratio or the true stresses for the entire duration of the test. Such data is essential, for instance, to develop models in finite element solvers (Quanjin et al., 2020; Rosas, 2019; Xu et al., 2019).

Thus, digital image correlation (DIC) methods are a promising alternative. This technique started to be developed in the 80s and consists of strain field measurement without contact with the surface of the structure, replacing strain gauges (Palanca et al., 2016; Victor et al., 2019). It has high sensitivity and can acquire information about deformation in several planes and axes, through cameras capable of registering dot patterns on the surface of the specimen. Subsequently, a software tracks the movement of these points (pixels) and performs strain calculations (D'Anna et al., 2021; Quanjin et al., 2020).

In this context, this study carried out the tensile characterization of two main polyurethane samples: one reinforced with E-type glass fiber and the other with $CaCO_3$ particles. In manufacturing, two different matrices were used, one petrochemical and another one natural, obtained from castor oil. With the increasing use of green alternatives, the number of applications of natural polymers has grown (Yates and Barlow, 2013), also highlighting the importance of studies that compare polymers obtained from these two different sources.

In the tests, DIC was also applied to calculate the Poisson's ratio and, subsequently, Scanning Electron Microscopy (SEM) analyzes were done to reveal bubbles inside the composite and to investigate the interface between the fibers and the matrix, a relevant aspect on the response of the composite, with premature failures occurring if the interaction between the phases does not provide good adhesion (da Silva et al., 2019; Ebnesajjad, 2014).

2. Methodology

2.1. Sample Manufacturing

For each sample, 5 Specimens were manufactured using bi-component polyurethanes and by two slightly different processes.

Firstly, with the SikaForce 7710L100 resin and later, using the Kehl AG101 resin. For both materials, the pre-cure, inside the molds, was carried out for approximately 1h30 at 50ºC and the sample dimensions were according to the ASTM D638 Type I dumbbell die, with a cross-section 3.2 mm thick and 13 mm width.

The SikaForce matrix, which presents a density of around 1.5 g/cm³ was prepared in a ratio (mass) of 100:19 and resulted in 13g specimens. In some samples, portions of unidirectional type E fiberglass roving were also added, forming FRC's.

The most important manufacturing steps are: the reagents (isocyanate and polyol) addition; the mixing and bubbles removal; resin pouring into the mold; a rigid plastic film placement; an acrylic plate and a metallic piece positioning above the mold (to ensure the correct thickness); cure; mold removal, finishing. Figure 1 shows, schematically, the most important steps to manufacture the specimens.

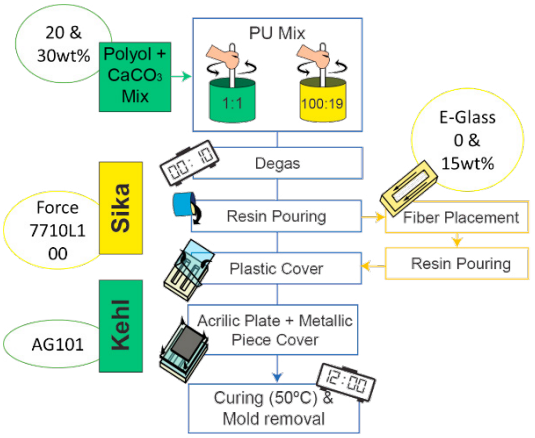

Fig. 1. Specimen manufacturing process.

In the FRC samples, a thin layer of resin was poured, over which 10 portions of fiber with a length equal to the total length of the specimen (165 mm) were placed. This amount of fiber represents approximately 15%wt of reinforcements in the transversal region of the sample. After the fiber being deposited, carefully aligned, and distributed; the mold was filled with resin and the other steps described above were done.

Regarding the Kehl matrix, with a 1:1 ratio, particulate reinforcements in calcium carbonate ($CaCO_3$ 99%, Synty) were also added. During the manufacturing, before mixing the components, the particulate was homogenized with the polyol in the proportions of 20 or 30%wt. However, for the proportion of 20%, two mixing methods were tested, the first one with the addition of the particulate to the polyol at room temperature and the second one with the polyol heating to 50ºC, reducing the viscosity and facilitating the process.

Table 1 summarizes all the manufactured materials and their respective composition:

Table 1: PU samples manufactured.

Group	Pu	FV	$CaCO_3$	Method
TK20C (1-5)	Kehl®	-	20%	Without poliol heating
TK20C (6-11)	Kehl®	-	20%	Poliol Heating at 50ºC
TK30C	Kehl®	-	30%	Poliol Heating at 50ºC
TS0F	Sika®	-	-	Standard (without heating)
TS15F	Sika®	15%	-	Standard (without heating)

2.2. Tensile Test

Two weeks after the specimen's manufacturing, the tensile tests were carried out according to ASTM D638 standard. The universal testing machine used was a Shimadzu Autograph AGS-X 10KN. The crosshead speed was constant and equal to 5mm/min, the gauge length was 115 mm and a 1N preload was applied.

The testing machine data acquisition system gave the crosshead displacement and the applied force. With this information, the engineering and true stresses and strains were calculated according to the equations in Table 2.

The modulus of elasticity was obtained from the slope of the linear region of the stress-strain curve.

Table 2: Equations for true and engineering stress and strain.

	Engineering	True
σ	$\sigma_e = \frac{P}{S_{t0}}$	$\sigma_r = \sigma_e(\varepsilon_e + 1)$
ε	$\varepsilon_e = \frac{l_i - l_0}{l_0}$	$\varepsilon_r = ln\left(\frac{l_i}{l_0}\right)$; $\varepsilon_r = ln(\frac{S_{t0}}{S_{ti}})^1$

2.3. Digital Image Correlation (DIC)

To apply the DIC method, images were acquired using a Canon® EOS 7D synchronized with a computer by the EOS Utility® software. A lighting system was set up and images were captured every 5 seconds.

All specimens were painted with a random pattern, as shown in Fig. 2 (a), and the photos obtained were processed in the Gom Correlate 2017 software.

Finally, the Poisson's ratio was calculated by the relationship between transverse and longitudinal strain obtained using “virtual strain gages” on Gom software.

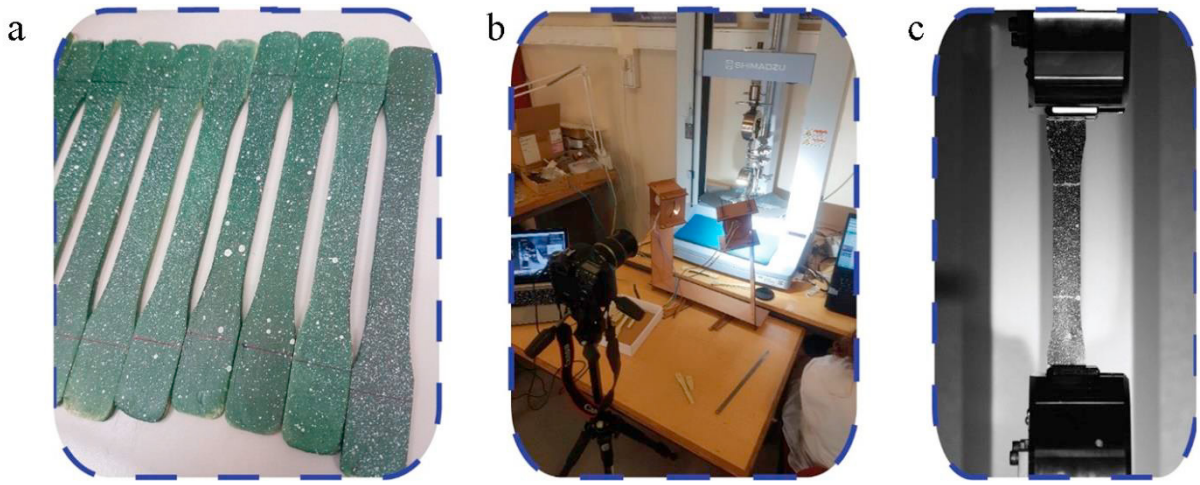

Fig. 2. (a) Samples panted with and random pattern; (b) Tensile test setup; (c) Image captured for the DIC process.

2.4. Scanning Electron Microscopy (SEM):

After the tensile tests, samples were selected to expose regions rich in reinforcements. The analyzed face was that one transversal to the tensile test axis, which means, SEM images should show breakage surface. In addition, the remaining faces of the samples were also cut until reaching surface areas of around 5mm²; the size necessary for placement in the microscopy equipment.

The images were taken using a Phenom Pro Desktop scanning electron microscope from Thermo Fisher Scientific (Eindhoven, The Netherlands), covering a sample region of approximately 1.25mm² and using a magnification around 215 times. The equipment was managed by its own software (Phenon ProSuite) and it was obtained images of the morphology, pores and fiber distribution in the samples.

After that, the images were digitally colorized to point out the main regions of interest.

3. Results and Discussion

3.1. Tensile Test

Table 3 shows the average results for each sample, wherein the maximum stress and strain showed were reached just before the rupture. The "t" subscribed index represents the true values, whereas the "e" index represents the engineering results.

Table 3: Tensile Test Results.

	σ_e [MPa]	ε_e [%]	σ_t [MPa]	ε_t [%]	E [MPa]
TK20C (1-5)	28.48±2.11	3.00±0.33	29.34±2.25	2.96±0.32	1144.44±139.95
TK20C (6-11)	31.41±3.66	2.83±0.11	32.30±3.80	2.77±0.11	1130.87±114.56
TK30C	36.20±5.40	2.63±0.20	37.15±5.55	2.59±0.20	1366.41±226.97
TS0F	10.55±1.65	7.85±1.76	11.42±2.00	7.75±1.93	330.03±72.18
TS15F	110.39±12.22	6.18±0.35	117.24±13.20	5.98±0.32	1869.63±121.18

In all cases, the true stress was higher than the engineering one, showing the effect of the section area changes during the test. For Kehl's material, the variation between these two maximum values (tensile strengths) was around 3%. This variation was bigger for specimens manufactured with Sika material, since they reached maximum loads with higher values of deformation, which also goes along with greater transverse deformation and, consequently, greater changes in the transverse area.

Samples from the TS0F group (PU Sika, without reinforcements) showed, on average, an 8.3% difference between these maximum stresses; where $\sigma_t = 11.42 \pm 2.00$MPa and $\sigma_e = 10.55 \pm 1.65$MPa for deformations around 7.8%; these data are consistent with the manufacturer's technical data sheet, which reports 13 MPa tensile strength, with an elongation at break of 8% (Sika, 2012).

The TS15F group (PU Sika with FV), due to the action of the fibers, deformed less (about 6%) and presented $\sigma_t = 117.24 \pm 13.20$MPa and $\sigma_e = 110.39 \pm 12.22$MPa.

Fig. 3 shows the average curves and deviations from the real stresses and strains. Samples from the TK groups (Kehl) showed maximum stresses higher than those from the TS0 group (Sika, without reinforcements).

Compared with pure Kehl resin (tensile strength of 20MPa), the particles also acted as reinforcement, being possible to notice an increase in strength (Kehl, n.d.). Because they have the same composition, all specimens with 20% CaCO3, manufactured without (TK20, 1-5) and with (TK20, 6-11) heating, had similar averages, with the maximum real stresses being 29.34 ± 2,25MPa and 32.30 ± 3.80MPa, respectively. However, the improvement in homogenization reduced the effects of carbonate as a stress raiser, resulting in a small increase in results.

In samples with 30% $CaCO_3$, the particulate became a reinforcement and the mean stress reached 37.15 ± 5.55MPa. However, as calcium carbonate was only mixed with the polyol, large additive amounts were difficult to homogenize (30% of the total mass represents, practically, the same amount of polyol and additive), justifying the increase in the results standard deviation, as shown in Figure 2b.

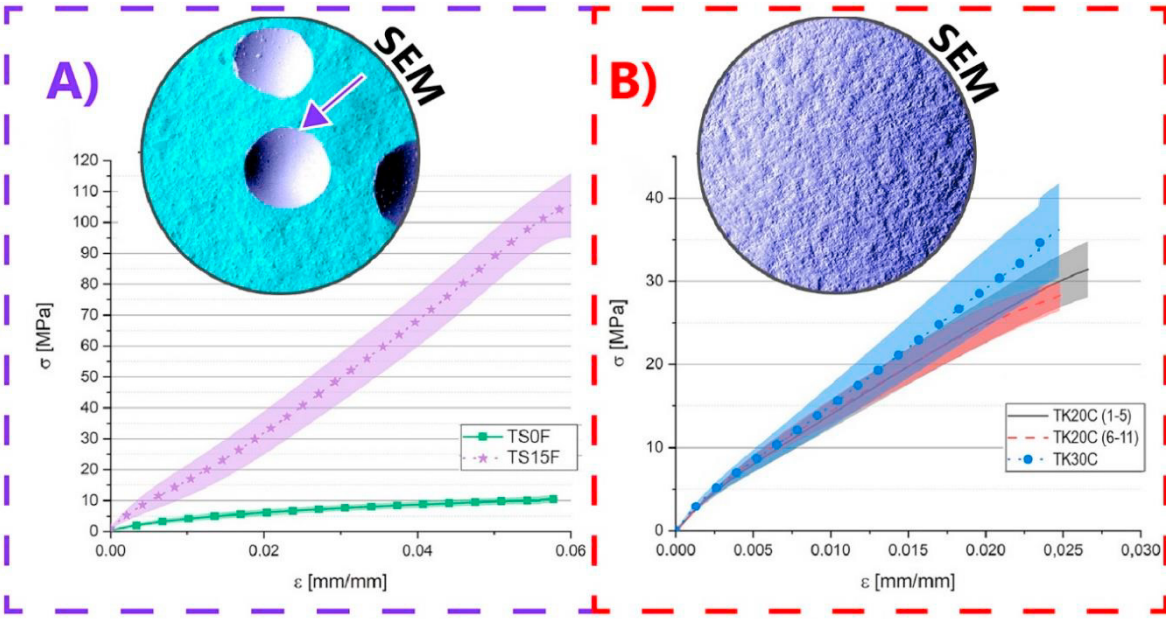

Fig. 3. Stress-strain curves and SEM colorized images: (a) Sika's PU samples; (b) Kehl's PU samples.

3.2. Digital Image Correlation

Silva et al, 2017, obtained the values of the Poisson's ratio for samples in pure polyurethane resin and reinforced with 7 layers of unidirectional cotton fiber. The matrix without reinforcements obtained average values of 0.440; in the composite, this value was reduced to 0.317 (Silva et al., 2017). Similarly, in the present work, the addition of fibers reduced the transversal deformation of the specimens, which decreased the Poisson's ratio from 0.433, in pure samples (TS0F), to 0.428 in the specimens of the TS15F group (15Wf% of FV).

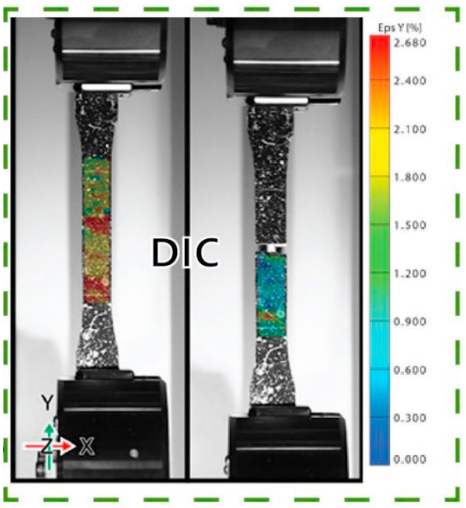

Fig. 4. Longitudinal strain field made by DIC showing the strain field before and after the breakage.

Table 4: Poisson's Ratio (υ)

	TK20C(1-5)	TK20C(6-11)	TK30C	TS0F	TS15F
υ	0.391±0.030	0.439±0.014	0.435±0.025	0.433±0.025	0.428±0.022

3.3. SEM

Microscopy images (Fig. 3) demonstrate that the samples manufactured with the Sika resin had a higher number of bubbles, which contributes to the reduction of the maximum supported stresses, since these pores, with dimensions of up to 25 µm, are the regions where the cracks started and headed the breakage.

Although heating facilitated the homogenization of Kehl resin, this process did not generate major differences in the presence or absence of empty regions in the material.

4. Conclusion

Mechanical properties of two different PU resins, pure and with the reinforcement of fibers or particles were studied through tensile. Also, DIC and SEM analyzes were performed, to obtain the Poisson Ratio and investigate the voids inside the material, respectively. Those studies showed that the tensile strength results were close to those declared by the manufacturer, with the fibers and particles acting as reinforcements. DIC proved to be an efficient method to obtain Poisson's ratio, and, in future works, it can be used to obtain the entire stress and strain curve. However, bubbles or voids had a great impact on the results of the Sika pure sample, which may have been responsible for the large standard deviation values presented by this group.

Acknowledgements

Funding

This research was partially funded through the base funding from the following research units: UIDB/00690/2020 (CIMO).

References

Boretos, J.W., Pierce, W.S., 1967. Segmented Polyurethane: A New Elastomer for Biomedical Applications. Science (80-.). 158, 1481–1482. https://doi.org/10.1126/science.158.3807.1481

Charlon, M., Heinrich, B., Matter, Y., Couzigné, E., Donnio, B., Avérous, L., 2014. Synthesis, structure and properties of fully biobased thermoplastic polyurethanes, obtained from a diisocyanate based on modified dimer fatty acids, and different renewable diols. Eur. Polym. J. 61, 197–205. https://doi.org/10.1016/j.eurpolymj.2014.10.012

Chattopadhyay, D.K., Raju, K.V.S.N., 2007. Structural engineering of polyurethane coatings for high performance applications. Prog. Polym. Sci. 32, 352–418. https://doi.org/10.1016/j.progpolymsci.2006.05.003

D'Anna, J., Amato, G., Chen, J.F., Minafò, G., La Mendola, L., 2021. Experimental application of digital image correlation for the tensile characterization of basalt FRCM composites. Constr. Build. Mater. 271, 121770. https://doi.org/10.1016/j.conbuildmat.2020.121770

Da Costa, R.R.C., De Medeiros, R., Ribeiro, M.L., Tita, V., 2017. Experimental and numerical analysis of single lap bonded joints: Epoxy and castor oil PU-glass fibre composites. J. Adhes. 93, 77–94. https://doi.org/10.1080/00218464.2016.1172212

da Silva, E.H.P., Almendro, E.B., da Silva, A.A.X., Waldow, G., Sales, F.C.P., de Moura, A.P., da Costa, R.R.C., 2019. Manufacture and Mechanical Behavior of Green Polymeric Composite Reinforced with Hydrated Cotton Fiber. J. Exp. Tech. Instrum. 2, 26–34. https://doi.org/10.30609/JETI.2019-7576

de Moura, A.P., da Silva, E.H., dos Santos, V.S., Galera, M.F., Sales, F.C., Elizario, S., de Moura, M.R., Rigo, V.A., da Costa, R.R., 2021. Structural and mechanical characterization of polyurethane-CaCO 3 composites synthesized at high calcium carbonate loading: An experimental and theoretical study. J. Compos. Mater. 002199832199641. https://doi.org/10.1177/0021998321996414

Ebnesajjad, S., 2014. Theories of Adhesion, in: Surface Treatment of Materials for Adhesive Bonding. Elsevier, pp. 77–91.

https://doi.org/10.1016/B978-0-323-26435-8.00005-8

Fu, C., Liu, J., Xia, H., Shen, L., 2015. Effect of structure on the properties of polyurethanes based on aromatic cardanol-based polyols prepared by thiol-ene coupling. Prog. Org. Coatings 83, 19–25. https://doi.org/10.1016/j.porgcoat.2015.01.020

Gao, X., Zhu, Y., Zhou, S., Gao, W., Wang, Z., Zhou, B., 2011. Preparation and characterization of well-dispersed waterborne polyurethane/CaCO3 nanocomposites. Colloids Surfaces A Physicochem. Eng. Asp. 377, 312–317. https://doi.org/10.1016/j.colsurfa.2011.01.025

Garcia, A., 2012. Ensaios Dos Materiais. LTC.

George, B., Suchithra, T.V., 2019. Plant-derived bioadhesives for wound dressing and drug delivery system. Fitoterapia 137, 104241. https://doi.org/10.1016/j.fitote.2019.104241

Kehl, n.d. Ficha técnica: Aglomerante Kehl Ag101.

Lazar, M.-A., Rotaru, H., Bâldea, I., Boşca, A.B., Berce, C.P., Prejmerean, C., Prodan, D., Câmpian, R.S., 2016. Evaluation of the Biocompatibility of New Fiber-Reinforced Composite Materials for Craniofacial Bone Reconstruction. J. Craniofac. Surg. 27, 1694–1699. https://doi.org/10.1097/SCS.0000000000002925

Lin, X., Xie, Q., Ma, C., Zhang, G., 2021. Self-healing, highly elastic and amphiphilic silicone-based polyurethane for antifouling coatings. J. Mater. Chem. B 9, 1384–1394. https://doi.org/10.1039/d0tb02465a

Palanca, M., Tozzi, G., Cristofolini, L., 2016. The use of digital image correlation in the biomechanical area: a review. Int. Biomech. 3, 1–21. https://doi.org/10.1080/23335432.2015.1117395

Quanjin, M., Rejab, M.R.M., Halim, Q., Merzuki, M.N.M., Darus, M.A.H., 2020. Experimental investigation of the tensile test using digital image correlation (DIC) method. Mater. Today Proc. 27, 757–763. https://doi.org/10.1016/j.matpr.2019.12.072

Reis, J.M.L., Chaves, F.L., da Costa Mattos, H.S., 2013. Tensile behaviour of glass fibre reinforced polyurethane at different strain rates. Mater. Des. 49, 192–196. https://doi.org/10.1016/j.matdes.2013.01.065

Rosas, J.D.L., 2019. IMPLEMENTAÇÃO DE UM SISTEMA PARA MEDIÇÃO DAS DEFORMAÇÕES NO PLANO PELA TÉCNICA DE CORRELAÇÃO DIGITAL DE IMAGEM. Politécnico do Porto.

Sales, F., Souza, A., Ariati, R., Noronha, V., Giovanetti, E., Lima, R., Ribeiro, J., 2021. Composite Material of PDMS with Interchangeable Transmittance: Study of Optical, Mechanical Properties and Wettability. J. Compos. Sci. 5, 110. https://doi.org/10.3390/jcs5040110

Sathishkumar, T., Satheeshkumar, S., Naveen, J., 2014. Glass fiber-reinforced polymer composites – a review. J. Reinf. Plast. Compos. 33, 1258–1275. https://doi.org/10.1177/0731684414530790

Sika, 2012. Ficha do produto: SikaForce®-7710 L100.

Silva, A.A.X., Silva, E., Janes, D., Domiciano, S., Costa, R., 2017. Mechanical Behavior of Composite of Polyurethane Reinforced with Cotton Fiber and Alumina Trihydrate. https://doi.org/10.26678/ABCM.COBEM2017.COB17-0501

Soric, Z., Galic, J., Rukavina, T., 2008. Determination of tensile strength of glass fiber straps. Mater. Struct. 41, 879–890. https://doi.org/10.1617/s11527-007-9291-4

Victor, A., Ribeiro, J., F. Araújo, F., 2019. Study of PDMS characterization and its applications in biomedicine: A review. J. Mech. Eng. Biomech. 4, 1–9. https://doi.org/10.24243/JMEB/4.1.163

Wang, W., Wang, C., 2012. Polyurethane for biomedical applications: A review of recent developments, in: The Design and Manufacture of Medical Devices. Elsevier, pp. 115–151. https://doi.org/10.1533/9781908818188.115

Xu, D., Cerbu, C., Wang, H., Rosca, I.C., 2019. Analysis of the hybrid composite materials reinforced with natural fibers considering digital image correlation (DIC) measurements. Mech. Mater. 135, 46–56. https://doi.org/10.1016/j.mechmat.2019.05.001

Yates, M.R., Barlow, C.Y., 2013. Life cycle assessments of biodegradable, commercial biopolymers—A critical review. Resour. Conserv. Recycl. 78, 54–66. https://doi.org/10.1016/j.resconrec.2013.06.010